Aeolian Research 29 (2017) 30–41

Contents lists available at ScienceDirect

Aeolian Research

journal homepage: www.elsevier.com/locate/aeolia

# Measurements of windblown dust characteristics and ocean fertilization potential: The ephemeral river valleys of Namibia

A.P. Dansie[a,*], G.F.S. Wiggs[a], D.S.G Thomas[a,b], R. Washington[c]

[a] School of Geography and the Environment, University of Oxford, Oxford OX1 3QY, UK
[b] Geography, Archaeology and Environmental Studies, University of the Witwatersrand, Johannesburg, South Africa
[c] Climate Research Lab, School of Geography and the Environment, University of Oxford, Oxford OX1 3QY, UK

ARTICLE INFO

*Keywords:*
Windblown dust
Sediment nutrients
Dry river valleys
Ocean fertilisation
Benguela Upwelling System

ABSTRACT

Delivery of nutrients to the ocean by mineral aerosol deposition involves complex biogeochemical interactions that include atmospheric processing, dissolution and biotic uptake of available nutrients in the surface waters. Research into the fertilization potential of aeolian dust is currently constrained by a lack of understanding of the nutrient composition and bioavailability in dust source areas. Further, research into hot-spots of dust emission has largely focused on paleo-lacustrine sources and pans, to the detriment of other potential sources such as ephemeral river valleys in desert regions. Here, we investigate the sediment characteristics and nutrient content of windblown and surface sediments of a largely overlooked southern African dust source, Namibia's ephemeral river valleys. We deployed monitoring equipment in three river valleys to capture deflated sediments and monitor airborne dust concentration and meteorological conditions throughout an annual dust season. Our results show that windblown dust within the river valleys is easily transportable offshore from Namibia over the Benguela Upwelling System, an intensely productive region of the South Atlantic Ocean. We demonstrate that the windblown dust contains iron, phosphorus and nitrogen nutrients, each of which may positively impact primary production rates when deposited in the complex upwelling system. The river valley dust has a significantly higher content of nutrients than either of southern Africa's major dry lake bed dust sources, Etosha and Makgadikgadi Pans. This aeolian work builds on previous source sediment findings proposing the ephemeral river valleys of Namibia as regionally important sources of dust with enhanced ocean fertilisation potential.

## 1. Introduction

Airborne mineral dust, with particles < 100 µm diameter (Ginoux et al., 2004; Maring et al., 2003; Tegen and Lacis, 1996), is a critical component of Earth System behaviour affecting atmospheric, oceanic and terrestrial processes. Presently dry or seasonally inundated lacustrine systems in drylands are widely identified as key sources of global dust (Jickells et al., 2005). These sources include both Quaternary lake basins, such as the Bodélé Depression, Chad (Washington et al., 2009; Todd et al., 2007); Makgadikgadi Pans in Botswana (Bryant et al., 2007), Etosha Pan in Namibia (Prospero et al., 2002), and Lake Eyre in Australia (McTainsh and Strong, 2007), and basins desiccated in the twentieth century by human activity such as the Aral Sea (Singer et al., 2003) and Owens Lake (Reid et al., 1994). Ephemeral dryland valleys in a range of global contexts have also been identified as important dust sources, including in Alaska (Muhs et al., 2016; Brungard et al., 2015), Antarctica (Bhattachan et al., 2015), Iraq, Kuwait, the UAE (Jish Prakash et al., 2015) and Namibia (Vickery et al., 2013).

Once airborne, mineral aerosols can travel considerable distances, with deposition occurring in oceans and over landmasses far from source. These dryland-sourced mineral aerosols have been estimated to account for 95% of atmospheric iron (Fe) (Mahowald et al., 2009) and 82% of atmospheric phosphorus (P) (Mahowald et al., 2008). This flux of nutrients from source to sink can have significant biological and ecological impacts. It has been proposed, for example, that the Amazon rainforest is dependent on phosphorus derived from mineral aerosols emanating from the Sahara (Swap et al., 2002), and that primary production in nutrient-limited regions of the open oceans derives Fe, P and N from dust inputs (Jickells and Moore, 2015). While uncertainties remain as to the precise biogeochemical roles of Fe, P and N across the global spectrum of marine sinks (Achterberg, 2014), the overall nutrient loading of dust is widely recognised as essential to marine productivity (Bouwman et al., 2013; Zehr and Kudela, 2011; Mahowald et al., 2008), and especially so in high nutrient, low chlorophyll (HNLC) zones (Jickells et al., 2014). The waters of large upwelling systems, biogeochemically-similar to HNLC zones, such as the Benguela

* Corresponding author at: School of Geography and the Environment, University of Oxford, Oxford OX1 3QY, UK.
*E-mail address:* a.dansie@oxfordalumni.org (A.P. Dansie).

http://dx.doi.org/10.1016/j.aeolia.2017.08.002
Received 7 January 2017; Received in revised form 27 July 2017; Accepted 30 July 2017
Available online 05 November 2017

upwelling system on Namibia's coast have similarly shown the capacity to be severely Fe-limited for primary production (Capone and Hutchins, 2013).

The ephemeral river valleys of Namibia are a prime example of a seasonal dryland dust emission source, with deflation due to strong easterly winds in the austral winter (Vickery and Eckardt, 2013). Visible on satellite imagery as distinct linear plumes (NASA, 2003), windblown dust frequently falls out over the surface of the South Atlantic (Stuut et al., 2002). The surface sediments in these ephemeral valleys have been shown to contain high levels of ocean-fertilising

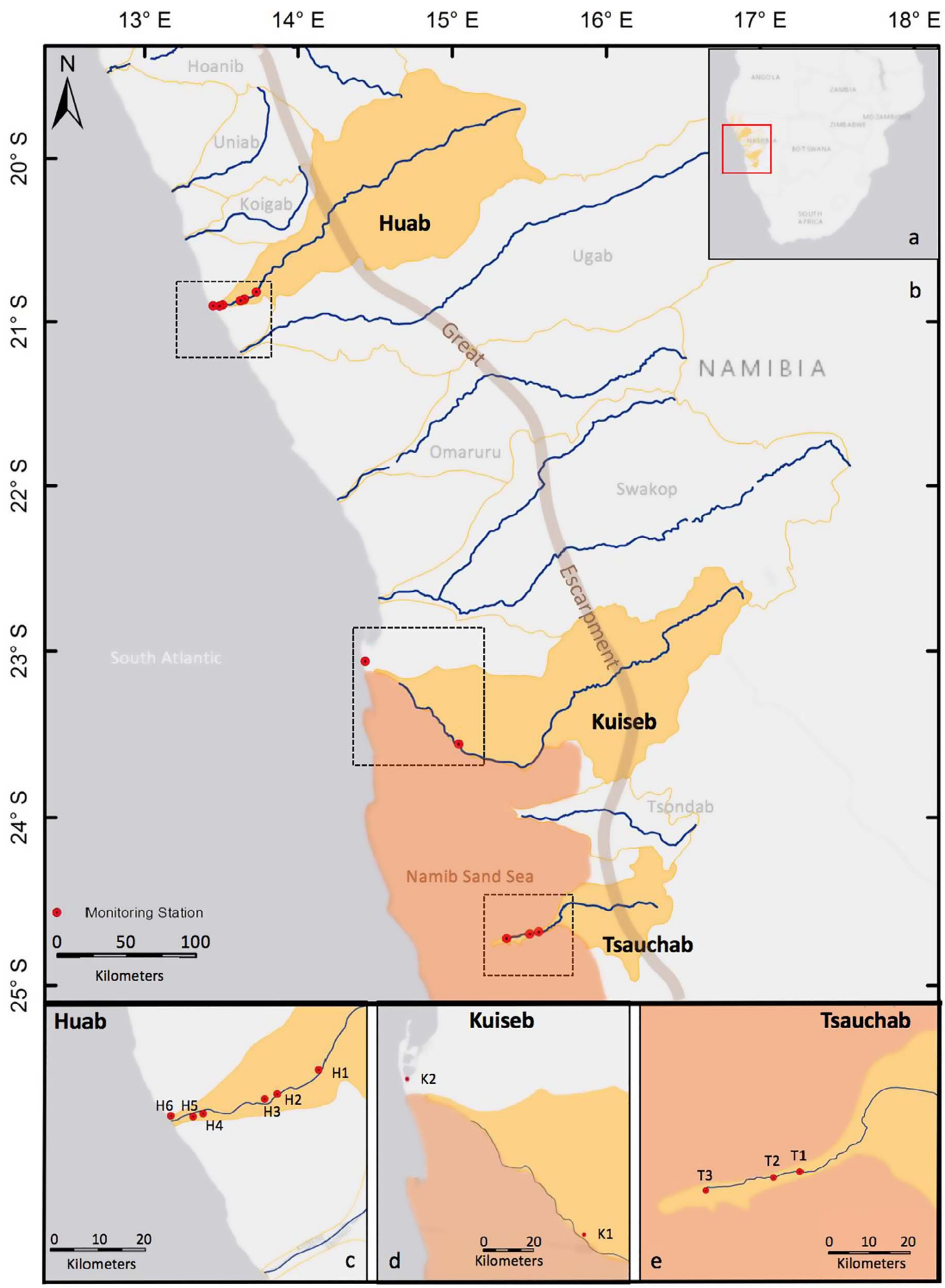


**Fig. 1.** (a) The ephemeral river valleys of western Namibia with (b) the location of the monitoring stations in the lower Huab, Kuiseb and Tsauchab river valleys. Station names are shown for the (c) Huab, (d) Kuiseb and (e) Tsauchab.

nutrients, most notably bioavailable Fe, (Dansie et al. 2017a), but as yet there are no measured data quantifying the physical characteristics, geo-chemistry or nutrient content of the windblown dust, and so the potential for fertilisation in the oceanic deposition region is unknown.

To address this data gap we monitored dust emission events in three Namibian river valleys during the austral winter of 2013 and sampled the windblown dust emitted from key emission sites within the lower valley systems. This paper determines for the first time the aerosol concentration, sediment characteristics and nutrient content of windblown dust emitted from Namibia's dry river valleys, and compares the nutrient content of the transported dust with those of the source material. The frequency of dust plumes observed using remote sensing during the field season is assessed, with a particular focus on identifying those observed to terminate over the South Atlantic. Together, these analyses provide the first evidence for the ocean fertilisation potential of mineral aerosols derived from the ephemeral river valleys of Namibia. It additionally provides a comparison to southern Africa's major dry lacustrine dust source areas of Etosha and the Makgadikgadi pan system.

## 2. Regional setting

The E-W aligned ephemeral river valleys of Namibia are located between latitudes 18°S and 25°S (Fig. 1a). The river valleys are sourced in the 1000 m high Great Escarpment (Morin et al., 2009) and flow through the 100–150 km wide Namib Desert to terminate in either the South Atlantic or Namib Sand Sea (Fig. 1b). The river channel width within the valley floor varies between 20 and 100 m, interchanging between stream and braided channel systems (Jacobsen et al., 1995), with the twelve catchments combined covering an area of 151,800 km$^2$. On the plateau and highlands above the escarpment the average annual rainfall reaches over 300 mm a year (Jacobsen et al., 1995). This can generate slope wash and colluvium movement in the upper watershed (Bierman and Caffee, 2001) that over time enters the ephemeral fluvial system and is subject to down-valley transport. Below the escarpment the valleys hold several metres of alluvial material that has accumulated in various phases during the Late Quaternary, notably in the last 40 ka (Stone and Thomas, 2013). Reworking and fluvial incision of this valley fill occurs during modern flood events that erode and reshape the channel through the valley floor. These ephemeral flows originate from precipitation in the upper catchment between January and March (Krapf et al., 2003), with pluvial activity having seen a modest increase compared to 8–9 ka ago (Eitel et al., 2001). Rainfall rarely occurs below the escarpment in the west with the Namib desert experiencing only 0–25 mm of annual precipitation which is mostly in the form of fog (Jacobson et al., 1995).

Regional atmospheric circulation patterns generate predominantly south-to-southwesterly trade winds over the dry river valley regions for most of the year (Lancaster, 1985). The notable exception to this general airflow pattern is the occurrence of strong east-to-northeasterly 'berg' winds during the austral winter months (Fryberger et al., 1979). These strong winds are caused by perturbations to the quasi-permanent continental high pressure cell by transient eddies, in the form of high pressure systems that ridge south of the African continent (Newell et al., 1972). The seasonal circulation also impacts localised diurnal wind patterns that are produced by a strong thermo-topographic coupling (Lindesay and Tyson, 1990) generating local nocturnal winds in winter that drain towards the coast (Tyson and Seely, 1980). The E-W alignment of the Namibian valleys may additionally funnel the regional easterly and more local winds, enhancing their ability to entrain valley floor sediments, a potential noted by Wiggs et al. (2002).

Namibia's offshore waters are dominated by the Benguela upwelling system, one of four Eastern Boundary Upwelling Systems (EBUS) globally which hosts the highest rates of primary production in the ocean (Toggweiler and Carson, 1995; Chavez and Barber, 1987). The upwelling of the Benguela is wind-driven by the regional alongshore southeast trade winds which cause the surface and subsurface waters to be driven offshore by Ekman Transport (Cosmic, 1987) and replaced by deep water conveyed to the surface (Shannon and Nelson, 1996). Upwelling of the Benguela system is by far the least seasonal of the four global EBUS (Chavez and Messié, 2009). The regional wind regime provides the explanation for this, with stabilisation of the anticyclonic wind pattern by a coast-to-Kalahari topographical gradient that reduces the seasonal variability of upwelling (Hay and Brock, 1992). Though seasonal fluctuation is minimal on a global comparison, the Benguela upwelling system is often separated into three zones according to variations in upwelling regimes; north, central, and south (Jury, 2012). The north and south Benguela upwelling zones are respectively bounded by the Angola and Agulhas Currents. These major ocean currents influence their adjacent upwelling zones with increased winter

**Table 1**
Deployed instrumentation.

| River Valley | Monitoring Station | Distance inland from terminus (km) | Location description (valley width) | DustTrak | BSNEs |
|---|---|---|---|---|---|
| Huab | H1 | 30.32 | Valley floor (970 m) | X | X |
| | H2 | 21.3 | Valley floor (1100 m) | X | X |
| | H3 | 18.70 | Valley floor (230 m) | – | X |
| | H4 | 9.18 | Valley floor (320 m) | X | X |
| | H5 | 4.09 | Valley floor (1360 m) | X | X |
| | H6 | 0.2 | River delta (2490 m) | – | X |
| Kuiseb | K1 | 84.1 | Gobabeb research station, northern valley edge 600 m from river channel | X | X |
| | K2 | 1.17 | River delta on artificial breakwater constructed for salt evaporation ponds | X | – |
| Tsauchab | T1 | 25.09 | Valley floor | X | X |
| | T2 | 19.54 | Valley floor | X | X |
| | T3 | 4.07 | Terminal clay pan | X | X |

upwelling observed in the northern zone (Gammelsrød et al., 1998), caused by the intrusion of tropical waters (Rouault, 2012), while increased summer upwelling is seen in the southern zone (Andrews and Hutchings, 1980). The central zone is the least fluctuating (Jury, 2012), often classified as continually upwelling (e.g. Goubanova et al. (2013)) due to perennially consistent SE Trade winds between 22 and 28°S (Shannon and Nelson, 1996). This is the most spatially relevant zone for our research as it lies contiguous with the most likely deposition region of the aeolian dust investigated.

## 3. Methods

### 3.1. Field stations

Three ephemeral river valleys were investigated in this study: the Huab and Kuiseb, which both terminate in the South Atlantic, and the Tsauchab, which terminates endoreically in the Namib Sand Sea (Fig. 1b). All three valleys had previously been identified as significant annual emitters of dust using remote sensing analysis (Vickery et al., 2013; Eckardt and Kuring, 2005). Such analysis of satellite imagery recognised that persistent sources of dust emission tended to be located in the lower (western) regions of the river valleys and generally no further than 100 km inland (Vickery and Eckardt, 2013). Informed by the work of Vickery and Eckardt (2013) we erected a total of eleven monitoring stations in the lower catchment areas of the three valley systems identified as frequent dust emitters (Fig. 1). The stations operated for 20 weeks between April and September 2013 (the known dust 'season', Vickery and Eckardt (2013)) with equipment set up for the collection of windblown dust samples and data on airborne dust concentration and meteorological conditions (Table 1 and Fig. 2). Six stations were set up in the Huab, two in the Kuiseb and three in the Tsauchab (Fig. 1c, d and e). Physical capture of horizontal dust flux was undertaken at ten stations (see Table 1) using Big Spring Number Eight (BSNE) aeolian sediment samplers erected in a vertical profile at heights of 0.25, 0.47, 0.89 and 1.68 m (Mendez et al., 2011; Fryrear, 1986). At nine sites (see Table 1) a DustTrak DRX aerosol monitor (Wang et al., 2009) was also erected at a height of 3.18 m. This instrument recorded PM1, PM2.5, PM5, PM10 and total suspended particulate (TSP) concentrations at two minute intervals throughout the

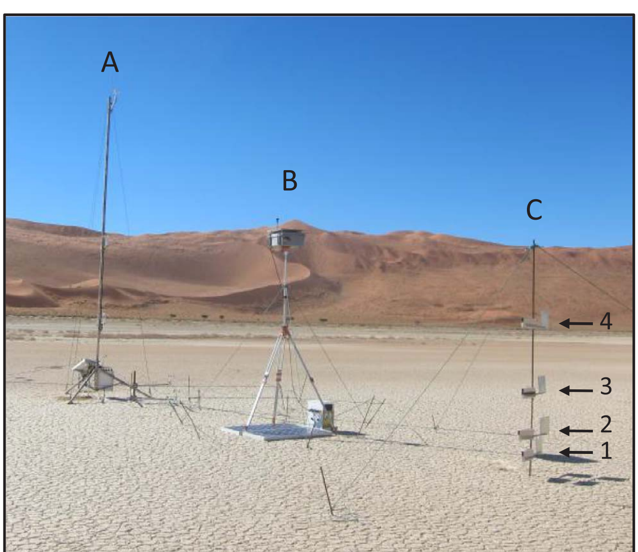


**Fig. 2.** Typical monitoring station consisting of (A) 6 metre (m) meteorological mast with anemometer and wind vane at 3.18 m, (B) DustTrak with inlet at 3.18 m, (C) BSNE horizontal flux collectors 1–4 with samplers set at 0.25, 0.47, 0.89 and 1.68 m collection heights respectively. The photograph shows station T3 as an example, where the transport direction of dust during strong easterly winds is from right to left in the photo.

study period. At each site an automatic weather station (AWS) was erected measuring average wind velocity and wind direction at 3.18 m height at an interval of one minute.

### 3.2. Sample collection

Samples of windblown dust in transport (collected by the BSNEs), surface sediment in the river valleys, and (for comparison) surface sediment of Etosha and Makgadikgadi pans were collected for particle size and chemical analysis. For collection of windblown dust, stations were visited monthly to empty BSNE traps and download meteorological data. Each BSNE was brushed into a pre-weighed ziplock bag using standard collection procedures (Zobeck et al., 2003; Fryrear, 1986).

Surface sediment samples were collected along transects adjacent to eight of the monitoring stations, as described by Dansie et al. (2017a), and data from their analyses are used here for comparison with the windblown dust samples collected from the BSNE traps. Surface samples were collected in a transect taken N-S perpendicular to the valley strike across the valley floor, modern channel deposits and, where present, any contemporary aeolian deposits.

Additionally, surface samples were collected from the Etosha and Makgadikgadi pans as part of a wider study. These samples are analysed here to allow a comparison of the ocean fertilisation potential of all the key southern African dust sources; the ephemeral river valleys, and Etosha and Makgadikgadi pans.

### 3.3. Sample analysis

Gravimetric weights were used to determine the scope of chemical (Fe, P, N) and physical (dry and wet grain size distribution) laboratory analyses that were possible on the windblown dust samples trapped in the BSNEs. A minimum of 18 g of sample was required for a full set of nutrient analyses to be undertaken, with a further minimum of 4 g needed for particle size measurements. A sufficient sample weight was not available from each individual BSNE sampler (a total of only 14% of samples met this criteria) so some within-site aggregation of samples was necessary. Samples from sites H2, H3 and H6 were sufficient to allow the sample from each individual collector to have a full set of nutrient and wet and dry grain size analyses. At T2 it was necessary to aggregate all four BSNEs in the vertical profile to generate sufficient mass for both chemical and grain size analysis. Remaining samples that did not reach the 18 g threshold were only analysed for dry-dispersion grain size (collections from the Huab (H2, H3, H4, H5, H6), Kuiseb (K1) and Tsauchab (T1, T2)). Two stations (H1 and T3) did not collect enough sample for any analyses to be carried out.

### 3.4. Chemical analyses

Sub-samples were analysed at the Kansas State University Soil Testing Laboratory where they were dried overnight in a 50 °C oven with the exception of sub-samples for iron analyses which were air-dried. Bioavailable $Fe^{2+}$ and $Fe^{3+}$ (combined) was extracted using DTPA (diethylenetriaminepentaacetic acid) then quantified using Flame Atomic Absorption spectrometry, following method described by Lindsay and Norvell (1978). Bioavailable P was determined using Mehlich III extraction (Mehlich, 1984) as described in Brown (1998). The inorganic nitrogen forms of ammonium ($NH_4^+$) and nitrate ($NO_3^-$) were extracted with 1 M of KCl for measurement in a flow analyser to determine ammonium and nitrate concentrations using colorimetric procedures, as detailed in Brown (1998). Total nitrogen (TN) and total phosphorus (TP) were determined using a modified Kjeldahl digestion followed by analysis of separate colorimetric reactions using a flow analyser (N as described by McLeod (1992) and P as described by Taylor (2000)).

### 3.5. Grain size analysis

Grain size data (volume weighted mean of particle diameter) were generated using a Malvern Mastersizer Hydro 2000 MU, with both dry and wet (disaggregated) methods being applied to splits of the same samples. Dry analysis represents the particle size distributions of samples as found in the field, preserving sediment pellets, peds and other aggregates, while wet analysis requires a breakdown of sediments into their individual-grain constituents. The terms 'sediment aggregates' and 'individual grains' are used to identify the results of dry and wet

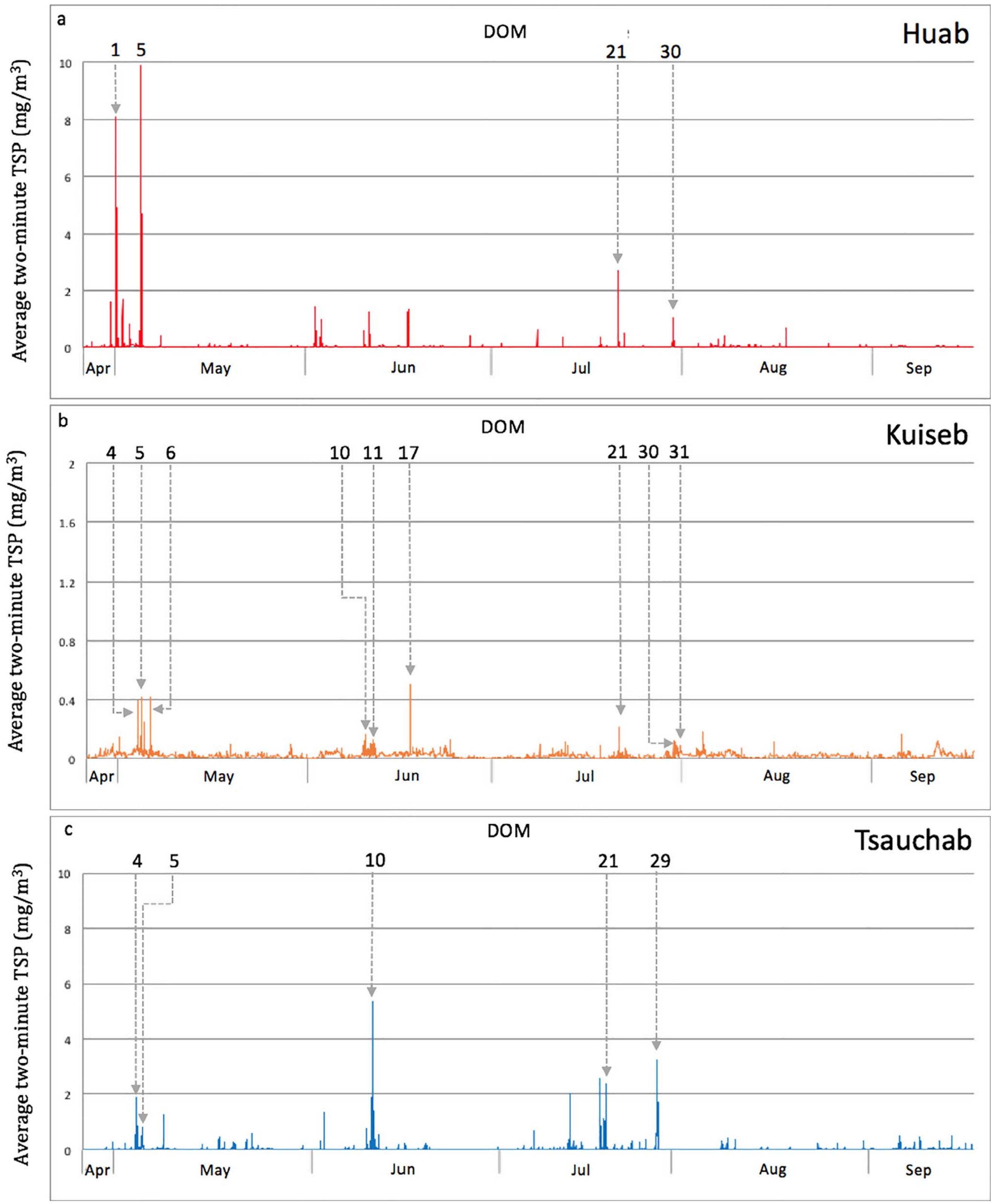


**Fig. 3.** Average two-minute TSP concentrations in the (a) Huab, (b) Kuiseb and (c) Tsauchab between April to September 2013 (recorded two-minute TSP concentrations at each station averaged within each river valley). Note differing y-axis scales. Dates that produced visible plumes off the coast identified with DOM (date of month).

**Table 2**
Airborne TSP concentrations (mg.m$^{-3}$) measured in the river valleys on dates of observed ocean-bound dust plumes (highlighted events as denoted in Fig. 3) with valley-averaged wind speed (ms$^{-1}$) recorded during the event and calculated daily wind speed average within each valley.

| Month | Day | Huab | Kuiseb | Tsauchab |
|---|---|---|---|---|
| May | 1 | **8.10**[a] (9.06[b], 4.94[c]) | - (9.53, 4.48) | - (3.31, 3.05) |
| | 4 | - (5.24, 3.87) | **0.41** (11.64, 7.80) | **1.88** (9.88, 6.98) |
| | 5 | **9.87** (10.52, 5.49) | **0.25** (8.18, 5.90) | **0.83** (8.39, 5.90) |
| | 6 | - (5.63, 4.25) | **0.42** (9.73, 6.15) | - (4.68, 3.78) |
| June | 10 | - (3.99, 3.10) | **0.16** (8.55, 7.47) | **5.34** (9.72, 7.73) |
| | 11 | - (5.63, 3.82) | **0.13** (3.95, 4.06) | - (5.55, 4.42) |
| | 17 | - (4.75, 3.33) | **0.51** (11.57, 6.61) | - (3.82, 3.54) |
| July | 21 | **2.72** (10.31, 5.81) | **0.22** (9.90, 7.07) | **2.38** (9.67, 6.71) |
| | 29 | - (5.79, 4.94) | - (7.97, 6.78) | **3.25** (10.25, 8.66) |
| | 30 | **1.04** (10.55, 6.69) | **0.12** (8.67, 6.62) | **~** (10.73, 8.07) |
| | 31 | - (5.00, 4.37) | **0.95** (8.04, 5.86) | - (4.91, 3.83) |

[a]Average two-minute TSP concentrations (mg.m$^{-3}$) in the river valleys (two-minute TSP concentration measurements at each station averaged within each valley) during dust events on dates of ocean-bound plume emission.
[b]Average wind speed (ms$^{-1}$) during recorded dust events in emitting valleys (cells highlighted) and for the matching period of time in non-emitting valley(s) (cells not highlighted).
[c]Daily average wind speed (ms$^{-1}$) within each river valley calculated from two-minute measurements.

analyses respectively.

For dry analysis samples were riffled to a weight of 0.1–3.5 g and analysed using a Malvern Mastersizer Scirocco 2000, using standard procedures (Malvern Instruments, 2007). Where required, samples were re-riffled to appropriate weights to ensure laser obscuration values were maintained between 1.0–3.5%. The analysis of one in ten samples was repeated to ensure reproducibility of results.

For wet analysis 3.0–5.0 g of sample was processed to remove salts and carbonates as described by Soukup et al. (2008). Oven-dried (40 °C) samples were ground using a mortar and pestle, split into sub-samples and suspended in a 1:1 solution of 50 g/L sodiumhexametaphosphate and DI water. The samples were then shaken for 4 h at 250 rpm and left to stand overnight. Grain size analysis was then performed using soil optimised procedures (Sperazza et al., 2004) with acceptable obscuration of 10–20%. Three measurements per sample were taken and the average calculated. Similar to the dry analyses, one in ten samples were repeated to ensure reproducibility of results.

### 3.6. Identification of dust plumes over the ocean

Visual inspection of satellite imagery was used to identify dust plumes emitted from the river valleys during the 20 weeks duration of the field deployment. Visual inspection of 15-min interval SEVIRI true colour and dust detection imagery (provided at http://www.fennec.imperial.ac.uk) and daily MODIS Aqua and Terra Corrective Reflectance (True Colour) accessed in the Earth Observing System Data and Information System (EOSDIS) (available at https://worldview.earthdata.nasa.gov) was undertaken for the period April to September 2013 inclusive.

## 4. Results and discussion

### 4.1. Dust emission events

During the course of field data collection a total of 18 dust events occurred that produced dust plumes extending over the ocean, as observed using EOSDIS and SEVIRI imagery. Airborne dust concentration data from the river valleys are shown in Fig. 3 with observed plumes over the ocean highlighted by date. Four of these major plumes

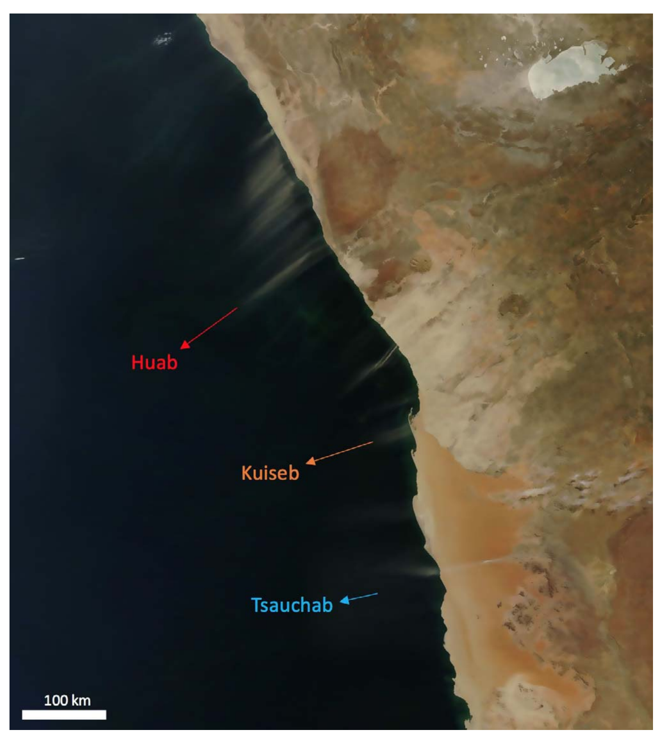


**Fig. 4.** Composite image of dust plumes emitted off the coast from the Huab and Kuiseb (5 May) and Tsauchab (29 July) taken from MODIS Terra Corrected Reflectance (True Colour) obtained from the Earth Observing System Data and Information System (EOSDIS) available at NASA Worldview (www.worldview.earthdata.nasa.gov).

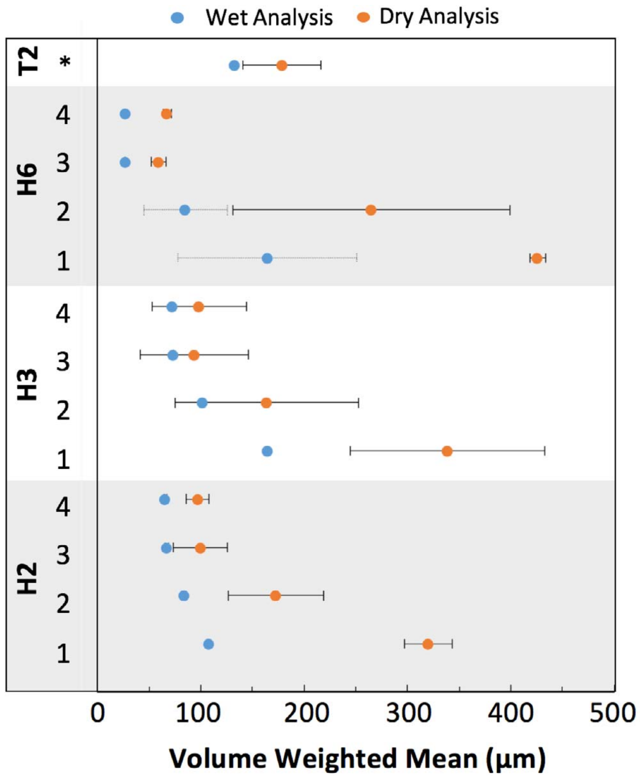


**Fig. 5.** Volume weighted mean grain size of wet and dry grain size distribution analyses from BSNE samplers in the Huab and Tsauchab (* T2 is combined BSNE 1, 2, 3 and 4 samplers) river valleys (averages calculated across multiple collections for H2 and H6. Horizontal bars show standard deviation where multiple collection dates were analysed (all dry analyses and only H2 and H6 for wet analyses). Standard deviation bars are too small to be observed for H2 (BSNE 1 = 2.32 μm, BSNE 2 = 2.31 μm, BSNE 3 = 1.62 μm, BSNE 4 = 1.24 μm) and BSNE 3 and 4 at H6 (0.33 and 0.06 μm respectively).

emanated from the Huab, nine from the Kuiseb and five from the Tsauchab.

The Huab was the dustiest river valley, with maximum two-minute average TSP concentrations reaching up to 9.87 mg $m^{-3}$ during emission events (see Table 2), compared to the maximum averages reached in the Kuiseb of 0.5 mg $m^{-3}$ and Tsauchab of 5.34 mg $m^{-3}$. Whilst the Kuiseb produced the greatest number of ocean-bound plumes, measured dust concentrations for each event in the Kuiseb were approximately an order of magnitude lower than values from the other valleys (Fig. 3). The relatively low dust concentrations recorded in the Kuiseb are likely to result partly from the locations of the two monitoring stations in this valley (see Fig. 1). For practical reasons, both stations in the Kuiseb were located on the edge of the river valley, rather than on the floor of the river valley. These stations therefore recorded dust already in transport, rather than dust concentrations at the site of actual emission on the valley floor. However, visible identification of dust plumes using satellite imagery showed that the Kuiseb site at the distal end of the valley (K2) was located within the transport pathway of all emitted plumes and so we have confidence that the measured data reflect true dust concentrations. Similarly, analysis of remote sensing imagery revealed that measurement sites in the Tsauchab and Huab were also within the transport pathway of emitted plumes in their respective valleys.

The most extensive dust events, where all three valleys produced dust plumes extending over the ocean, were on the 5 May, 21 July and 30 July 2013. Wind speed was between 8.18 and 10.73 $ms^{-1}$ in all valleys during these emission events (Table 2). Differences in key emission dates between the river valleys were also observed (Fig. 3 and Table 2). The reason for this was variations in easterly wind strengths through the region on dust-emitting days. Daily averages were calculated (Table 2) and show the non-emitting valleys all recording below 5 $ms^{-1}$ daily averages compared to 90% of dust-emitting valleys reporting a daily average >5 $ms^{-1}$. Note that no TSP data in the Tsauchab is shown for this latter event in Fig. 3c and Table 2 due to field equipment failure.

The observed variance in dust emission days between river valleys is most prominent on 1 May when only the Huab produced a distinct dust plume. The average wind strength during the dust-event, across all monitoring stations in the Huab, was 9.06 $ms^{-1}$ compared to a lower maximum of 3.31 $ms^{-1}$ in the non-emitting Tsauchab and 9.53 $ms^{-1}$ in the minimally-emitting Kuiseb (Fig. 3b, Table 2). In spatial contrast, June saw emissions from the Kuiseb and Tsauchab on the 10 and the Kuiseb only on the 11 and 17 (Fig. 3) with none from the Huab. Wind speed measurements during these dust events and calculated daily average wind speeds both show elevated wind strength in the southern two valleys (event averages up to 9.72 $ms^{-1}$ and 11.57 $ms^{-1}$) compared to the Huab during the same period (3.99–5.63 $ms^{-1}$). Over 100% increases in recorded wind speed between emitting and non-emitting valleys are shown on 10 and 17 June (Table 2).

Wind conditions clearly show localised differences between the

**Table 3**
Average grain size class distribution (%, dry analysis) for aggregated BSNE samples and potential transport distances as observed in the literature.

| River Valley | BSNE | Grain size fraction (μm) | | | | | | |
|---|---|---|---|---|---|---|---|---|
| | | 0–20 | 20–65 | 65–100 | 100–150 | 150–350 | 350–1000 | 1000–2000 |
| Huab | 4 | 11.60 | 32.10 | 28.41 | 15.05 | 7.83 | 1.34 | 3.67 |
| | 3 | 13.30 | 30.78 | 28.89 | 15.73 | 8.46 | 1.35 | 1.49 |
| | 2 | 8.79 | 20.11 | 22.18 | 14.01 | 16.85 | 14.13 | 3.94 |
| | 1 | 5.12 | 10.55 | 11.69 | 9.40 | 31.64 | 27.21 | 4.39 |
| Kuiseb | 4 | 0.85 | 15.40 | 25.60 | 21.73 | 29.90 | 6.52 | 0.00 |
| | 3 | 0.49 | 13.07 | 27.73 | 24.49 | 29.27 | 4.94 | 0.00 |
| | 2 | 0.54 | 9.52 | 17.68 | 16.35 | 22.60 | 10.70 | 22.61 |
| | 1 | 0.67 | 9.50 | 20.25 | 20.89 | 33.64 | 9.07 | 5.97 |
| Tsauchab | 4 | 4.51 | 29.21 | 29.03 | 16.15 | 7.77 | 1.19 | 12.14 |
| | 3 | 4.14 | 23.87 | 27.80 | 17.10 | 9.35 | 2.09 | 15.64 |
| | 2 | 4.95 | 21.09 | 27.86 | 19.66 | 20.12 | 6.32 | 0.00 |
| | 1 | 1.41 | 7.72 | 11.94 | 12.87 | 43.46 | 21.57 | 1.04 |
| | | > 4000 | 3000 | 650 | | | | |
| | | Transport potential (km)[a] | | | | | | |

[a]Empirical evidence for >4000 km, 3000 km and 650 km as provided by Prospero et al. (1970), Middleton and Goudie (2001), and Glaccum and Prospero (1980) respectively.

river valleys (Table 2) and these play a definitive role in the dust emission potential of each valley (Fig. 3). A composite image of dust emission events (accounting for cloud coverage) for 5 May and 29 July is shown in Fig. 4. This clearly demonstrates that these large events enable the transport of significant amounts of valley-derived dust over the ocean. All dust events with plumes observed to reach the ocean occurred before midday during strong (11–12 $ms^{-1}$) easterly winds, (Preston-Whyte et al., 1994; Lindesay and Tyson, 1990), Over-ocean dust events were observed to peak at 10:30 UTC on each emission date with plumes first reaching the coast at dawn (05:45 UTC) and becoming separated from the mainland at around 10:15 UTC, matching the temporal characteristics (Lancaster, 1985; Fryberger et al., 1979) of the thermos-topographic induced (Lindesay and Tyson, 1990) winds.

No dust plumes were seen to reach the ocean in August or September, with only small events evident in Fig. 3 and wind speed daily averages only exceeding 5 $ms^{-1}$ once in each of the Kuiseb (5.09 $ms^{-1}$ on 15 September) and Tsauchab (5.94 $ms^{-1}$ on 5 Sep). The Huab, however, recorded daily averages exceeding 5 $ms^{-1}$ on 15 days in August and September but this was not matched with either notable increases in TSP concentrations (Fig. 3a) or observed dust plumes. The absence of dust plumes at this time was confirmed by visual inspection of 15-min interval SEVIRI true colour and dust detection imagery (provided at http://www.fennec.imperial.ac.uk) and daily true colour MODIS Aqua and Terra EOSDIS images (https://worldview.earthdata.nasa.gov) which showed the coast dominated by cloud and fog during these months (34 fog/cloud total obscuration days out of the 46 monitored days from 1 August to 16 September). Easterly winds were less prevalent in these months and regionally recirculated air movements carrying biomass haze were identifiable (EOSDIS), traversing the ephemeral river region from the NW to E direction. This recirculation is a known-occurrence during these months caused by the semi-permanent continental high pressure cell that provides significant influence on the subtropical atmospheric circulation in the region (Tyson and D'Abreton, 1998) and is not conducive to dust emission over the South Atlantic from the ephemeral valleys.

Our analysis of both field data and satellite imagery confirms that windblown dust derived from the ephemeral river valleys is transported offshore during large easterly wind events. During the course of our field experiment each valley emitted between 4 and 9 of such over-ocean plumes. This seasonal frequency of large events is similar to that found by the remote sensing analyses of Eckardt and Kuring (2005) who investigated 150 plumes emitted from the river valleys and coastal sabkhas between 1998 and 2001 and also the higher resolution study of Vickery et al. (2013) which identified 111 river valley plumes between 2005 and 2008. This was more than the combined emission frequency from southern Africa's major paleolacustrine sources which, in the same high-resolution study, saw 32 plume emissions from Etosha and 53 from Makgadikgadi pans (Vickery et al., 2013). Our results provide the first TSP concentration measurements of dust-plumes from the river valleys that have only previously been defined in terms of emission frequency from remote sensing observations. This is an important first step towards characterising the magnitude of aeolian sediment flux from the river valleys to the ocean each year.

### 4.2. Grain size of windblown dust

Results from the dry and wet grain size analyses for the Huab (Fig. 5) show that the windblown dust is comprised of both individual grains and sediment aggregates formed through the cohesion of finer sediments. Large (up to 340 μm) aggregates such as crust pieces captured in the lowest BSNE (BSNE 1) are seen to be lifted up to 0.25 m height and aggregates up to 170 μm up to 0.47 m (BNSE 2, Fig. 5). Once in momentum, these large aggregates are subject to in-air collisions and impacts with the surrounding terrain, resulting in aggregate disintegration that forms both smaller fragments and release of individual parent grains (Shao, 2004) that are able to be transported at greater heights, with the higher placed BSNE traps collecting greater proportions of finer dust particles (Table 3) (Dong et al., 2003; Greeley et al., 1983). Both individual grains and sediment aggregates show a volume weighted mean size of 100 μm or less in the upper BSNEs (BSNE 4 in Fig. 5), a size range common to mineral aerosols (Ginoux et al., 2004; Arimoto et al., 1997; Tegen and Lacis, 1996). This demonstrates that the observed dust plumes (Fig. 4) would contain both individual grains and sediment aggregates, with a greater proportion of the former. The surface sediments of accumulated alluvium that form the valley floors comprise 40% individual grains $<100$ μm (Dansie et al. 2017a), providing an abundant source of fine unconsolidated sediment for wind erosion.

The grain size of the eroded sediment is a major determinant of the transport distance potential of the airborne dust. The in situ grain size fractions of the captured dust in all three river valleys (H2, H3, H4, H5, H6, K1, T1, T2 (Fig.1a-c), Table 3) demonstrate that it is clearly transportable over the distance from the inland monitoring stations (Fig. 1) to the ocean, extending over 100 km from the coast as observed by visible plumes (Fig. 4). It is noted that the delivery of nutrients could be enhanced in aggregated particles (Fig. 5, dry analysis, Table 3)

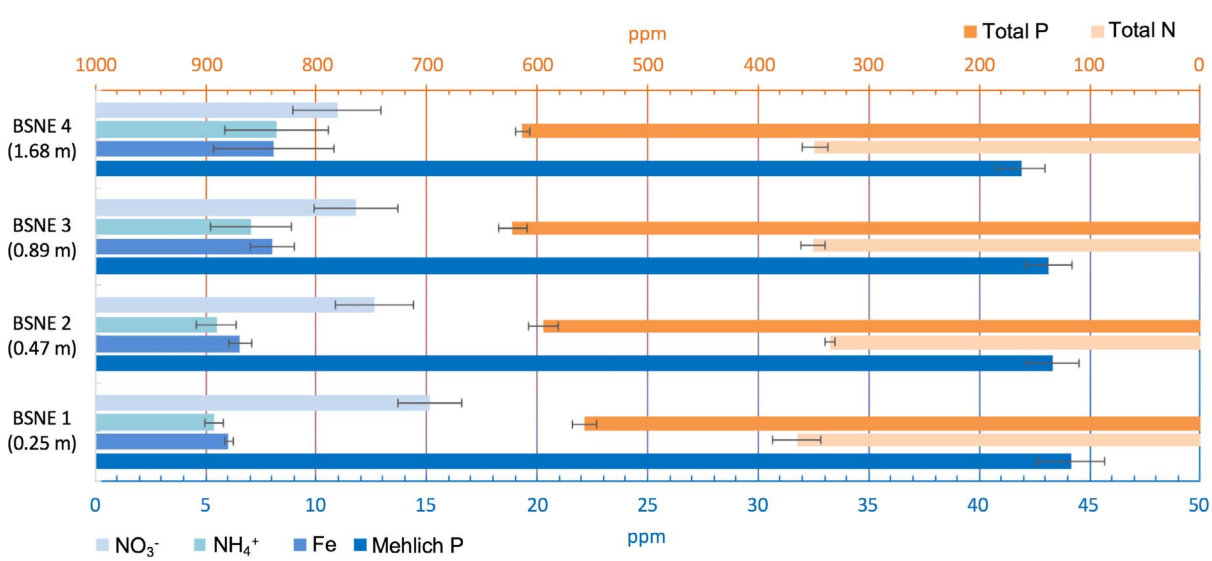


**Fig. 6.** Mean nitrate ($NO_3^-$), ammonium ($NH_4^+$), bioavailable iron (Fe), bioavailable P (Mehlich P), total nitrogen (Total N) and total phosphorus (Total P) concentrations according to BSNE height from Huab 2 (three collections) and Huab 3 (one collection). Bars indicate standard deviation. Huab 6 was excluded due to the potential influence of ocean spray.

where internal nutrients, having not been exposed to the same degree of weathering as individual particles and therefore more bioavailable (Shi et al., 2011), are also released.

### 4.3. Nutrient content of windblown dust

The geochemistry of windblown dust is shown in Fig. 6. Our results show that entrained sediment collected at all BSNE heights between 0.25 and 1.68 m contain both bioavailable Fe and P and N-based macronutrients and could therefore contribute to the nutrient-loading of observed dust plumes. It is difficult to compare these data with other studies of airborne nutrient concentration measurements, especially the bioavailable fractions, because of the varying analytical extraction methods that produce varying results (López-García et al., 2017; Anderson et al., 2010) with differing detection limits and analytical errors (Formenti et al., 2011). Bioavailable fractions of mineral aerosol Fe, the ocean fertilising nutrient that has seen the most research attention, vary widely in the literature from 0.01 to 80% (Mahowald et al., 2009). Measurements are highly influenced by the laboratory techniques used, for example, both the acidity of the leaching solution and the digestion time increases the Fe dissolution (Boyd et al., 2010a; Gaspari et al., 2006; Guieu and Thomas, 1996), preventing their meaningful comparison. Call for the standardisation of the methodologies has been made previously to improve the data sets available to biogeochemical models (Boyd et al., 2010b), and this would also greatly assist in the inter-comparison of nutrient content of dust from different sources.

Noting this, some trends of nutrient content varying according to height are observed (Fig. 6). Concentrations of bioavailable Fe are seen to increase (33%) between the near-surface (0.25 m) and top (1.68 m) BSNE, although it is noted this is within the standard deviation, which itself increases with collection height. TN concentrations are uniform across collection heights (Fig. 6) with variations observed in the bioavailable N fractions. Ammonium ($NH_4^+$) concentrations are seen to increase (53%) between BSNE 1 and 4 similar to Fe. Nitrate ($NO_3^-$) shows an inverse relationship with 15 ppm reported in BSNE 1 compared to 11 ppm in BSNE 4. Both $NH_4^+$ and $NO_3^-$ are highly accessible for phytoplankton uptake (Moore et al., 2013; Boyd et al., 2010a; Michaels et al., 1996), with $NH_4^+$ also having the potential for conversion into nitrate ($NO_3^-$) following oceanic deposition by ammonia-oxidising bacteria (Kowalchuk and Stephen, 2001). TP concentration is similarly shown to modestly increase with collection height (Fig. 6). An

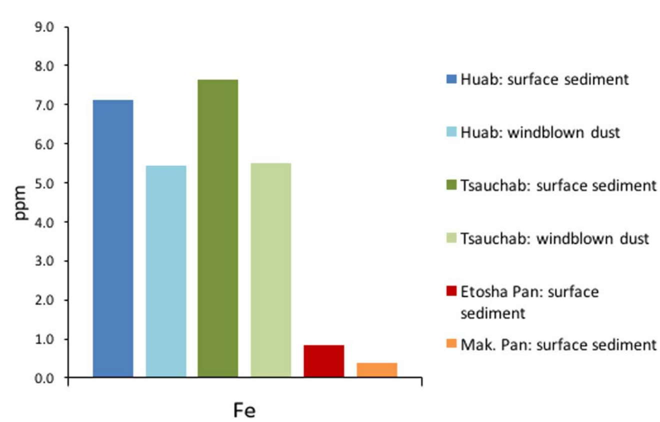


**Fig. 7.** Mean bioavailable Fe content of surface and windblown dust from the Huab and Tsauchab monitoring stations. Comparison with the regionally significant Etosha and Makgadikgadi pan dust sources is provided, see Dansie et al. (2017a). The mean values in the river valley surface sediment shown in Figs. 7 and 8 are calculated using all surface sediment samples of valley fill, channel fines and channel coarse material presented in Dansie et al. (2017a). Mean results of the BSNE samples are calculated using collected samples from H2, H3, and H6 and S2. The mean concentrations include all samples collected from the four BSNE collection heights, representing all material entrained between 0.25 and 1.68 m high during deflation events.

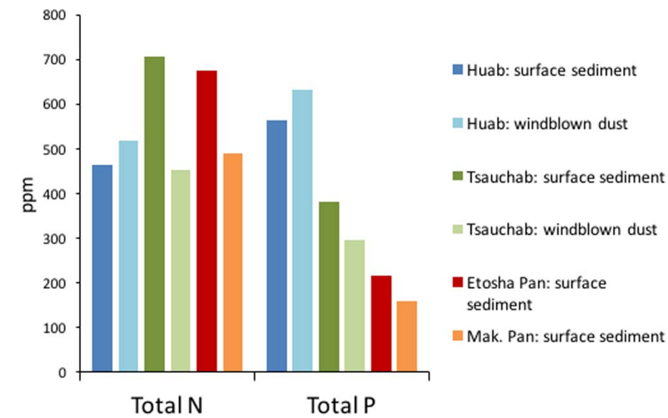


**Fig. 8.** Mean Total N and Total P content of surface and windblown dust from the Huab and Tsauchab monitoring stations. Comparison with the regionally significant Etosha and Makgadikgadi pan dust sources is provided, see Dansie et al. (2017a)). Mean concentrations calculated as described for Fig. 7.

average TP content of 720 ppm is assumed in global dust models (Myriokefalitakis et al., 2016; Wang et al., 2015; Brahney et al., 2015), which is higher than that reported here (maximum of 622 ppm in BSNE 3, Fig. 6), but significant geographical variation of this value is known to exist globally (Mahowald et al., 2008) and, more recently, demonstrated across key emission areas previously considered homogenous in modeling assessments of nutrient flux (i.e. the Sahara (Gross et al., 2016)).

Our data show that the windblown dust we collected from the ephemeral river valleys of Namibia contain the micronutrient Fe and P and N macronutrients, all of which are known to facilitate phytoplanktonic growth in ocean waters (Moore et al., 2013; Jickells et al., 2005; Boyd et al., 2000). The relative importance of each nutrient for ocean fertilisation depends on the biogeochemical conditions and phytoplankton community species composition of the depositional waters (Hecky and Kilham, 1988; Tilman et al., 1982), which varies geographically and seasonally (Cetinić et al., 2015; Edwards et al., 2013). The nutrient(s) responsible for triggering phytoplanktonic growth, or limiting growth *in absentia*, across the Benguela upwelling system are not fully understood but insights can be found elsewhere. It is known that Fe limitation affects productivity in EBUS (Hutchins et al., 2002; Bruland et al., 2001) where the vertical transport of macronutrient-rich waters can create near-shore Fe-limited conditions similar to those found in the HNLC waters of the open ocean (Capone and Hutchins, 2013). Farther offshore from Namibia (−13.3°N, 0.0 °E), ocean waters have been shown to be co-limited by Fe and N (Moore et al., 2013). N limitation can both be alleviated through the direct input of bioavailable N compounds, or through P and Fe where these nutrients are limiting microbial nitrogen fixation (Mills et al., 2004). Therefore, in the case of phytoplanktonic growth off Namibia's coast being either Fe-limited, P + N limited (e.g. Tyrrell (1999)), or a combination of both (e.g. Bracken et al. (2015)), these conditions could be mediated by aeolian deposition of mineral aerosols from Namibia's river valleys.

### 4.4. The regional fertilisation potential of windblown dust from the ephemeral river valleys

The fertilisation potential of the windblown dust can be compared to previous reporting of source sediments (Dansie et al. 2017a) and the importance of these river valleys as a source of aeolian fertilisation considered in a southern African context; this comparison is possible due to identical laboratory analyses of surface sediment samples from the river valley source sediments and Etosha and Makgadikgadi pans, as described in Dansie et al. (2017a).

Results in Fig. 7 show that bioavailable Fe concentrations of windblown dust in the river valleys are similar to those previously reported for the in-situ sampled surface sediments (Dansie et al. 2017a). The average bioavailable Fe content of deflated dust was 5.5 ppm in both the Huab and Tsauchab, compared to slightly higher levels of 7.1 ppm and 7.5 ppm in the Huab and Tsauchab surface sediments respectively (Fig. 7). The dust-emitting lower reaches of the Huab and Tsauchab river valleys are separated N-S by five other river valleys over a distance of ~460 km (Fig. 1b). It may therefore be inferred that windblown dust in the other Namibian river valleys might contain similar bioavailable Fe concentrations. This is further supported by Dansie et al. (2017b), who showed that sediment in the dust-emitting lower river valley reaches contained enriched levels of bioavailable Fe irrespective of watershed geology or land use (see Dansie et al. 2017b). This suggests that Namibia's ephemeral river valleys, stretching for a combined ~800 km along the coast (Fig. 1a), may be considered an extensive and regionally significant dust source for productivity in the Benguela region of the southern Atlantic in comparison to southern Africa's major paleolacustrine dust sources (Fig. 7).

Fig. 8 shows the total concentration of N and P macronutrients in windblown dust compared to in-situ sampled surface sediment. Total P concentrations are shown to be comparable between surface sediment and windblown dust samples within each river valley. A similar relationship is seen for Total N in the Huab but not in the Tsauchab. Dansie et al. (2017b) showed that Total N concentrations in the fluvial deposits in the Tsauchab were the highest of all three river valleys. The endoreic terminus of the Tsauchab enhances water accumulation following channel flow, influencing infiltration rates and subsequently microbiological processes that are heavily dependant on soil moisture and environmental conditions (Kidron et al., 2015). Increased N levels have previously been correlated with hydrological flows in these Namibian rivers (e.g. Jacobson et al. (2000)). The macronutrient loading of river valley dust shows that P is found in higher concentrations than in Etosha and Makgadikgadi pan sources. The P content of the river valley surface sediment and windblown dust is therefore also considered to be regionally significant but not to the extent shown for bioavailable Fe. River valley N concentrations are not considered regionally significant compared to the pans.

## 5. Conclusion

This study has shown that windblown dust collected in the river valleys is largely comprised of particle size ranges that are easily transportable to the ocean and carries levels of nutrients similar to the in-valley source sediment, considered significant and of overall greater primary production potential than either of southern Africa's major pan sources. We have shown that the ocean-bound dust contains Fe, P and N, each of which may remedy offshore ocean nutrient limitations thereby impacting primary productivity in the Benguela upwelling system. The abundant source material in the river valleys and the replenishing and reworking mechanisms of ephemeral flows support consideration of the ephemeral river valleys as a significant dust source of nutrient rich, fine grained sediment suited for aeolian transport offshore. We observed that the valleys each emitted between 4 and 9 plumes that terminated over the ocean during the 2013 dust season, similar to the seasonal frequency previously reported by remote sensing investigations. Extrapolation of our results across the twelve Namibian ephemeral river valleys would identify an 800 km N-S coastal region that contains numerous source areas of mineral aerosols with elevated bioavailable nutrients: we hypothesise that this coastal dust source may be an important contributor to the adjacent ocean nutrient cycle. Interplay between the seasonal cycle of dust emission and the annual upwelling regime of the Benguela system would impact primary production. This is proposed to play an underreported and important role in the wind-driven spatial and temporal marine productivity cycles off the coast of Namibia.

## Acknowledgements

The authors gratefully acknowledge the support by the Clarendon Fund and Oxford University Press for this research and the John Fell Fund for providing partial support of fieldwork activities. Dr. James King and Ass. Prof. Frank Eckardt are thanked for their major contributions and tireless efforts during the field season and follow-on support. Dr. Sebastian Engelstäder is thanked for his collaboration in the field. We are very thankful to the Gobabeb Research and Training Centre for their comprehensive support and for hosting one of the monitoring stations. We thank the Namibian Ministry of Environment and Tourism for all their support and assistance, especially with access to field sites permitted under permit number 1788/2013. This research has been carried out in collaboration with the Natural Environment Research Council grant NE/H021841/1.

## References

Achterberg, E.P., 2014. Grand challenges in marine biogeochemistry. Front. Marine Sci. 1, 7.
Anderson, L., Faul, K., Paytan, A., 2010. Phosphorus associations in aerosols: What can they tell us about P bioavailability? Mar. Chem. 120 (1), 44–56.
Andrews, W., Hutchings, L., 1980. Upwelling in the southern Benguela current. Prog. Oceanogr. 9 (1), 1–81.
Arimoto, R., Ray, B., Lewis, N., Tomza, U., Duce, R., 1997. Mass-particle size distributions of atmospheric dust and the dry deposition of dust to the remote ocean. J. Geophys. Res.: Atmos. (1984–2012) 102 (D13), 15867–15874.
Bhattachan, A., Wang, L., Miller, M.F., Licht, K.J., D'Odorico, P., 2015. Antarctica's dry valleys: a potential source of soluble iron to the southern ocean? Geophys. Res. Lett. 42 (6), 1912–1918.
Bierman, P.R., Caffee, M., 2001. Slow rates of rock surface erosion and sediment production across the Namib Desert and escarpment, southern Africa. Am. J. Sci. 301 (4–5), 326–358.
Bouwman, A., Bierkens, M., Griffioen, J., Hefting, M., Middelburg, J., Middelkoop, H., Slomp, C., 2013. Nutrient dynamics, transfer and retention along the aquatic continuum from land to ocean: towards integration of ecological and biogeochemical models. Biogeosciences 10 (1), 1–22.
Boyd, P.W., Strzepek, R., Fu, F., Hutchins, D.A., 2010a. Environmental control of open-ocean phytoplankton groups: Now and in the future. Limnol. Oceanogr. 55 (3), 1353.
Boyd, P.W., Watson, A.J., Law, C.S., Abraham, E.R., Trull, T., Murdoch, R., Bakker, D.C., Bowie, A.R., Buesseler, K., Chang, H., 2000. A mesoscale phytoplankton bloom in the polar Southern Ocean stimulated by iron fertilization. Nature 407 (6805), 695–702.
Boyd, P., Mackie, D., Hunter, K., 2010b. Aerosol iron deposition to the surface ocean—modes of iron supply and biological responses. Mar. Chem. 120 (1), 128–143.
Bracken, M.E., Hillebrand, H., Borer, E.T., Seabloom, E.W., Cebrian, J., Cleland, E.E., Elser, J.J., Gruner, D.S., Harpole, W.S., Ngai, J.T., 2015. Signatures of nutrient limitation and co-limitation: responses of autotroph internal nutrient concentrations to nitrogen and phosphorus additions. Oikos 124 (2), 113–121.
Brahney, J., Mahowald, N., Ward, D.S., Ballantyne, A.P., Neff, J.C., 2015. Is atmospheric phosphorus pollution altering global alpine Lake stoichiometry? Global Biogeochem. Cycles 29 (9), 1369–1383.
Brown, J.R., 1998. Recommended Chemical Soil Test Procedures for the North Central Region. Missouri Agricultural Experiment Station, University of Missouri-Columbia.
Bruland, K.W., Rue, E.L., Smith, G.J., 2001. Iron and macronutrients in California coastal upwelling regimes: implications for diatom blooms. Limnol. Oceanogr. 46 (7), 1661–1674.
Brungard, C.W., Boettinger, J.L., Hipps, L.E., 2015. Wind erosion potential of lacustrine and alluvial soils before and after disturbance in the eastern Great Basin, USA: Estimating threshold friction velocity using easier-to-measure soil properties. Aeolian Res. 18, 185–203.
Bryant, R.G., Bigg, G.R., Mahowald, N.M., Eckardt, F.D., Ross, S.G., 2007. Dust emission response to climate in southern Africa. J. Geophys. Res.: Atmos. 112 (D9).
Capone, D.G., Hutchins, D.A., 2013. Microbial biogeochemistry of coastal upwelling regimes in a changing ocean. Nat. Geosci. 6 (9), 711–717.
Cetinić, I., Perry, M., D'Asaro, E., Briggs, N., Poulton, N., Sieracki, M., Lee, C., 2015. A simple optical index shows spatial and temporal heterogeneity in phytoplankton community composition during the 2008 North Atlantic Bloom Experiment. Biogeosciences 12 (7), 2179–2194.
Chavez, F.P., Barber, R.T., 1987. An estimate of new production in the equatorial Pacific. Deep Sea Res. Part A. Oceanographic Res. Pap. 34 (7), 1229–1243.
Chavez, F.P., Messié, M., 2009. A comparison of eastern boundary upwelling ecosystems. Prog. Oceanogr. 83 (1), 80–96.
COSMIC, P., 1987. Wind-driven ocean currents and Ekman transport.
Dansie, A., Thomas, D., Wiggs, G., Munkittrick, K., 2017b. Spatial variability of ocean fertilising nutrients in the dust-emitting ephemeral river catchments of Namibia. Earth Surf. Proc. Land in press.
Dansie, A., Wiggs, G., Thomas, D., 2017a. Iron and nutrient content of wind-erodible sediment in the ephemeral river valleys of Namibia. Geomorphology 290, 335–346.
Dong, Z., Liu, X., Wang, H., Zhao, A., Wang, X., 2003. The flux profile of a blowing sand cloud: a wind tunnel investigation. Geomorphology 49 (3), 219–230.

Eckardt, F., Kuring, N., 2005. SeaWiFS identifies dust sources in the Namib Desert. Int. J. Remote Sens. 26 (19), 4159–4167.
Edwards, K.F., Litchman, E., Klausmeier, C.A., 2013. Functional traits explain phytoplankton community structure and seasonal dynamics in a marine ecosystem. Ecol. Lett. 16 (1), 56–63.
Eitel, B.W., Dieter BlümelHüser, K., Mauz, B., 2001. Dust and loessic alluvial deposits in Northwestern Namibia (Damaraland, Kaokoveld): sedimentology and palaeoclimatic evidence based on luminescence data. Quaternary Int. 76, 57–65.
Formenti, P., Schütz, L., Balkanski, Y., Desboeufs, K., Ebert, M., Kandler, K., Petzold, A., Scheuvens, D., Weinbruch, S., Zhang, D., 2011. Recent progress in understanding physical and chemical properties of African and Asian mineral dust. Atmos. Chem. Phys. 11 (16), 8231–8256.
Fryberger, S.G., Ahlbrandt, T.S., Andrews, S., 1979. Origin, Sedimentary Features, and Significance of Low-Angle Eolian. J. Sediment. Res. 49 (3).
Fryrear, D., 1986. A field dust sampler. J. Soil Water Conserv. 41 (2), 117–120.
Gammelsrød, T., Bartholomae, C., Boyer, D., Filipe, V., O'Toole, M., 1998. Intrusion of warm surface water along the Angolan-Namibian coast in February–March 1995: the 1995 Benguela Niño. S. Afr. J. Mar. Sci. 19 (1), 41–56.
Gaspari, V., Barbante, C., Cozzi, G., Cescon, P., Boutron, C.F., Gabrielli, P., Capodaglio, G., Ferrari, C., Petit, J.R., Delmonte, B., 2006. Atmospheric iron fluxes over the last deglaciation: Climatic implications. Geophys. Res. Lett. 33 (3).
Ginoux, P., Prospero, J.M., Torres, O., Chin, M., 2004. Long-term simulation of global dust distribution with the GOCART model: correlation with North Atlantic Oscillation. Environ. Modell. Softw. 19 (2), 113–128.
Glaccum, R.A., Prospero, J.M., 1980. Saharan aerosols over the tropical North Atlantic—Mineralogy. Mar. Geol. 37 (3), 295–321.
Goubanova, K., Illig, S., Machu, E., Garçon, V., Dewitte, B., 2013. SST subseasonal variability in the central Benguela upwelling system as inferred from satellite observations (1999–2009). J. Geophys. Re.: Oceans 118 (9), 4092–4110.
Greeley, R., Williams, S.H., Marshall, J.R., 1983. Velocities of Windblown Particles in Saltation: Preliminary Laboratory and Field Measurements. Dev. Sedimentol. 38, 133–148.
Gross, A., Palchan, D., Krom, M., Angert, A., 2016. Elemental and isotopic composition of surface soils from key Saharan dust sources. Chem. Geol. 442, 54–61.
Guieu, C., Thomas, A., 1996. Saharan aerosols: From the soil to the ocean. In: The impact of desert dust across the Mediterranean. Springer, pp. 207–216.
Hay, W.W., Brock, J.C., 1992. Temporal variation in intensity of upwelling off southwest Africa. Geolog. Soc., London, Sp. Publ. 64 (1), 463–497.
Hecky, R., Kilham, P., 1988. Nutrient limitation of phytoplankton in freshwater and marine environments: a review of recent evidence on the effects of enrichment. Limnol. Oceanogr. 33 (4), 796–822.
Hutchins, D., Hare, C., Weaver, R., Zhang, Y., Firme, G., Ditullio, G., Alm, M., Riseman, S., Maucher, J., Geesey, M., 2002. Phytoplankton iron limitation in the Humboldt Current and Peru Upwelling. Limnol. Oceanogr. 47 (4), 997–1011.
Jacobson, P.J., Jacobson, K.N., Seely, M.K., 1995. Ephemeral rivers and their catchments: sustaining people and development in western Namibia. Desert Res. Foundation Namibia.
Jacobson, P., Jacobson, K., Angermeier, P., Cherry, D., 2000. Hydrologic influences on soil properties along ephemeral rivers in the Namib Desert. J. Arid Environ. 45 (1), 21–34.
Jickells, T., An, Z., Andersen, K.K., Baker, A., Bergametti, G., Brooks, N., Cao, J., Boyd, P., Duce, R., Hunter, K., 2005. Global iron connections between desert dust, ocean biogeochemistry, and climate. Science 308 (5718), 67–71.
Jickells, T., Boyd, P., Hunter, K.A., 2014. Biogeochemical Impacts of Dust on the Global Carbon Cycle. Mineral Dust. Springer 359–384.
Jickells, T., Moore, C.M., 2015. The Importance of Atmospheric Deposition for Ocean Productivity. Annu. Rev. Ecol. Evol. Syst. 46, 481–501.
Jish Prakash, P., Stenchikov, G., Kalenderski, S., Osipov, S., Bangalath, H., 2015. The impact of dust storms on the Arabian Peninsula and the Red Sea. At. Chem. Phys. 15 (1), 199–222.
Jury, M.R., 2012. Physical oceanographic influences on Central Benguela fish catch. Earth Interactions 16 (6), 1–15.
Kidron, G.J., Posmanik, R., Brunner, T., Nejidat, A., 2015. Spatial abundance of microbial nitrogen-transforming genes and inorganic nitrogen in biocrusts along a transect of an arid sand dune in the Negev Desert. Soil Biol. Biochem. 83, 150–159.
Kowalchuk, G.A., Stephen, J.R., 2001. Ammonia-oxidizing bacteria: a model for molecular microbial ecology. Ann. Rev. Microbiol. 55 (1), 485–529.
Krapf, C.B., Stollhofen, H., Stanistreet, I.G., 2003. Contrasting styles of ephemeral river systems and their interaction with dunes of the Skeleton Coast erg (Namibia). Quatern. Int. 104 (1), 41–52.
Lancaster, N., 1985. Winds and sand movements in the Namib sand sea. Earth Surf. Proc. Land. 10 (6), 607–619.
Lindesay, J., Tyson, P., 1990. Climate and near-surface airflow over the central Namib. Namib Ecol. 25, 27–37.
Lindsay, W.L., Norvell, W.A., 1978. Development of a DTPA soil test for zinc, iron, manganese, and copper. Soil Sci. Soc. Am. J. 42 (3), 421–428.
López-García, P., Gelado-Caballero, M.D., Collado-Sánchez, C., Hernández-Brito, J.J., 2017. Solubility of aerosol trace elements: Sources and deposition fluxes in the Canary Region. Atmos. Environ. 148, 167–174.
Mahowald, N.M., Engelstaedter, S., Luo, C., Sealy, A., Artaxo, P., Benitez-Nelson, C., Bonnet, S., Chen, Y., Chuang, P.Y., Cohen, D.D., 2009. Atmospheric iron deposition: global distribution, variability, and human perturbations. Ann. Rev. Marine Sci. 1, 245–278.
Mahowald, N., Jickells, T.D., Baker, A.R., Artaxo, P., Benitez-Nelson, C.R., Bergametti, G., Bond, T.C., Chen, Y., Cohen, D.D., Herut, B., 2008. Global distribution of atmospheric phosphorus sources, concentrations and deposition rates, and anthropogenic impacts. Global Biogeochem. Cy 22 (4).
Malvern Instruments, 2007. Scirocco 2000 User Manual. MAN0386 1.0 edn. Worcestershire, UK: Malvern Instruments Ltd.
Maring, H., Savoie, D., Izaguirre, M., Custals, L., Reid, J., 2003. Mineral dust aerosol size distribution change during atmospheric transport. J. Geophys. Res.: Atmos. 108 (D19).
McLeod, S., 1992. Determination of total soil and plant nitrogen using a micro-distillation unit in a continuous flow analyzer. Anal. Chim. Acta 266 (1), 113–117.
McTainsh, G., Strong, C., 2007. The role of aeolian dust in ecosystems. Geomorphology 89 (1), 39–54.
Mehlich, A., 1984. Mehlich 3 soil test extractant: a modification of Mehlich 2 extractant. Commun. Soil Sci. Plant Anal. 15 (12), 1409–1416.
Mendez, M.J., Funk, R., Buschiazzo, D.E., 2011. Field wind erosion measurements with big spring number eight (bsne) and modified wilson and cook (mwac) samplers. Geomorphology 129 (1), 43–48.
Michaels, A., Olson, D., Sarmiento, J., Ammerman, J., Fanning, K., Jahnke, R., Knap, A., Lipschultz, F., Prospero, J., 1996. Inputs, losses and transformations of nitrogen and phosphorus in the pelagic North Atlantic Ocean. In: Nitrogen Cycling in the North Atlantic Ocean and Its Watersheds. Springer, pp. 181–226.
Middleton, N.J., Goudie, A.S., 2001. Saharan dust: sources and trajectories. Trans. Inst. British Geographers 26 (2), 165–181.
Mills, M.M., Ridame, C., Davey, M., la Roche, J., Geider, R.J., 2004. Iron and phosphorus co-limit nitrogen fixation in the eastern tropical North Atlantic. Nature 429 (6989), 292–294.
Moore, C., Mills, M., Arrigo, K., Berman-Frank, I., Bopp, L., Boyd, P., Galbraith, E., Geider, R.J., Guieu, C., Jaccard, S., 2013. Processes and patterns of oceanic nutrient limitation. Nat. Geosci. 6 (9), 701–710.
Morin, E., Grodek, T., Dahan, O., Benito, G., Kulls, C., Jacoby, Y., van Langenhove, G., Seely, M., Enzel, Y., 2009. Flood routing and alluvial aquifer recharge along the ephemeral arid Kuiseb River. Namibia. J. Hydrol. 368 (1), 262–275.
Muhs, D.R., Budahn, J.R., Skipp, G.L., McGeehin, J.P., 2016. Geochemical evidence for seasonal controls on the transportation of Holocene loess, Matanuska Valley, southern Alaska, USA. Aeolian Res. 21, 61–73.
Myriokefalitakis, S., Nenes, A., Baker, A.R., Mihalopoulos, N., Kanakidou, M., 2016. Bioavailable atmospheric phosphorous supply to the global ocean: a 3-D global modelling study. Biogeosciences.
NASA, 2003-last update, Visible Earth: Streamers of Dust off Namibia. Available: http://visibleearth.nasa.gov/view.php?id=11657 [2/26/2013, 2013].
Newell, R.E., Kidson, J.W., Vincent, D.G. and Boer, G.J., 1972. General circulation of the tropical atmosphere and interactions with extratropical latitudes. vol. 1.
Preston-Whyte, R., Diab, R., Sokolic, F., 1994. Thermo-topographically induced winds in the boundary layer over the Etosha Pan. South African Geog. J. 76 (2), 59–62.
Prospero, J.M., Bonatti, E., Schubert, C., Carlson, T.N., 1970. Dust in the Caribbean atmosphere traced to an African dust storm. Earth Planet. Sci. Lett. 9 (3), 287–293.
Prospero, J.M., Ginoux, P., Torres, O., Nicholson, S.E., Gill, T.E., 2002. Environmental characterization of global sources of atmospheric soil dust identified with the Nimbus 7 Total Ozone Mapping Spectrometer (TOMS) absorbing aerosol product. Rev. Geophys. 40 (1).
Reid, J.S., Flocchini, R.G., Cahill, T.A., Ruth, R.S., Salgado, D.P., 1994. Local meteorological, transport, and source aerosol characteristics of late autumn Owens Lake (dry) dust storms. Atmos. Environ. 28 (9), 1699–1706.
Rouault, M., 2012. Bi-annual intrusion of tropical water in the northern Benguela upwelling. Geophys. Res. Lett. 39 (12).
Shannon, L., Nelson, G., 1996. The Benguela: large scale features and processes and system variability. South Atlantic. Springer 163–210.
Shao, Y., 2004. Simplification of a dust emission scheme and comparison with data. J. Geophys. Res.: Atmos. 109 (D10).
Shi, Z.M.D., Krom, S., Bonneville, A.R., Baker, C., Drake, N., Mann, G., Carslaw, K., Mcquaid, J.B., Jickells, T., 2011. Influence of chemical weathering and aging of iron oxides on the potential iron solubility of Saharan dust during simulated atmospheric processing. Global Biogeochem. Cycles 25 (2).
Singer, A., Zobeck, T., Poberezsky, L., Argaman, E., 2003. The PM 10 and PM 2 5 dust generation potential of soils/sediments in the Southern Aral Sea Basin. Uzbekistan. J. Arid Environ. 54 (4), 705–728.
Soukup, D.A., Buck, B.J., Harris, W., 2008. Preparing soils for mineralogical analyses. In: Ulery, A.L., Drees, L.R. (Eds.), Methods of Soil Analysis, Part 5 – Mineralogical Methods. Soil Science Society of America, Inc., Madison, Wisconsin, USA, pp. 13–31.
Sperazza, M., Moore, J.N., Hendrix, M.S., 2004. High-resolution particle size analysis of naturally occurring very fine-grained sediment through laser diffractometry. J. Sediment. Res. 74 (5), 736–743.
Stone, A., Thomas, D., 2013. Casting new light on late Quaternary environmental and palaeohydrological change in the Namib Desert: A review of the application of optically stimulated luminescence in the region. J. Arid Environ. 93, 40–58.
Stuut, J.W., Prins, M.A., Schneider, R.R., Weltje, G.J., Jansen, J., Postma, G., 2002. A 300-kyr record of aridity and wind strength in southwestern Africa: inferences from grain-size distributions of sediments on Walvis Ridge. SE Atlantic. Marine Geol. 180 (1), 221–233.
Swap, R., Garstang, M., Greco, S., Talbot, R., Kållberg, P., 2002. Saharan dust in the Amazon Basin. Tellus B 44 (2), 133–149.
Taylor, M., 2000. Determination of total phosphorus in soil using simple Kjeldahl digestion. Commun. Soil Sci. Plan. Anal. 31 (15–16), 2665–2670.
Tegen, I., Lacis, A.A., 1996. Modeling of particle size distribution and its influence on the radiative properties of mineral dust aerosol. J. Geophys. Res.: Atmos. (1984–2012) 101 (D14), 19237–19244.
Tilman, D., Kilham, S.S., Kilham, P., 1982. Phytoplankton community ecology: the role of limiting nutrients. Annu. Rev. Ecol. Syst. 13, 349–372.

Todd, M.C., Washington, R., Martins, J.V., Dubovik, O., Lizcano, G., M'Bainayel, S., Engelstaedter, S., 2007. Mineral dust emission from the Bodélé Depression nothern Chad, during BoDEx 2005. J. Geophys. Res. D: Atmos. 112 (6).
Toggweiler, J., Carson, S., 1995. What are upwelling systems contributing to the ocean's carbon and nutrient budgets? Environ. Sci. Res. Rep. ES 18, 337–360.
Tyrrell, T., 1999. The relative influences of nitrogen and phosphorus on oceanic primary production. Nature 400 (6744), 525–531.
Tyson, P., D'Abreton, P., 1998. Transport and recirculation of aerosols off Southern Africa—macroscale plume structure. Atmos. Environ. 32 (9), 1511–1524.
Tyson, P., Seely, M., 1980. Local winds over the central Namib. S. Afr. Geogr. J. 62 (2), 135–150.
Vickery, K.J., Eckardt, F.D., 2013. Dust emission controls on the lower Kuiseb River valley, Central Namib. Aeolian Res. 10, 125–133.
Vickery, K.J., Eckardt, F.D., Bryant, R.G., 2013. A sub-basin scale dust plume source frequency inventory for southern Africa, 2005–2008. Geophys. Res. Lett. 40 (19), 5274–5279.
Wang, R., Balkanski, Y., Boucher, O., Ciais, P., Peñuelas, J., Tao, S., 2015. Significant contribution of combustion-related emissions to the atmospheric phosphorus budget. Nat. Geosci. 8 (1), 48–54.
Wang, X., Chancellor, G., Evenstad, J., Farnsworth, J.E., Hase, A., Olson, G.M., Sreenath, A., Agarwal, J.K., 2009. A novel optical instrument for estimating size segregated aerosol mass concentration in real time. Aerosol Sci. Technol. 43 (9), 939–950.
Washington, R., Bouet, C., Cautenet, G., Mackenzie, E., Ashpole, I., Engelstaedter, S., Lizcano, G., Henderson, G.M., Schepanski, K., Tegen, I., 2009. Dust as a tipping element: the Bodele Depression, Chad. Proc. Nat. Acad. Sci. U.S.A. 106 (49), 20564–20571.
Wiggs, G., Bullard, J., Garvey, B., Castro, I., 2002. Interactions between airflow and valley topography with implications for aeolian sediment transport. Phys. Geogr. 23 (5), 366–380.
Zehr, J.P., Kudela, R.M., 2011. Nitrogen cycle of the open ocean: from genes to ecosystems. Ann. Rev. Marine Sci. 3, 197–225.
Zobeck, T.M., Sterk, G., Funk, R., Rajot, J.L., Stout, J.E., van Pelt, R.S., 2003. Measurement and data analysis methods for field-scale wind erosion studies and model validation. Earth Surf. Proc. Land. 28 (11), 1163–1188.